Cell

A Translational Profiling Approach for the Molecular Characterization of CNS Cell Types

Myriam Heiman,[1] Anne Schaefer,[1] Shiaoching Gong,[2] Jayms D. Peterson,[5] Michelle Day,[5] Keri E. Ramsey,[6] Mayte Suárez-Fariñas,[4] Cordelia Schwarz,[3] Dietrich A. Stephan,[6] D. James Surmeier,[5] Paul Greengard,[1] and Nathaniel Heintz[2,3,*]

[1]Laboratory of Molecular and Cellular Neuroscience
[2]GENSAT Project
[3]Laboratory of Molecular Biology, Howard Hughes Medical Institute
[4]The Rockefeller University Hospital
The Rockefeller University, 1230 York Avenue, New York, NY 10065, USA
[5]Department of Physiology, Feinberg School of Medicine, Northwestern University, 303 East Chicago Avenue, Chicago, IL 60611, USA
[6]Neurogenomics Division, Translational Genomics Research Institute, 445 North 5th Street, Phoenix, AZ 85004, USA
*Correspondence: heintz@mail.rockefeller.edu
DOI 10.1016/j.cell.2008.10.028

SUMMARY

The cellular heterogeneity of the brain confounds efforts to elucidate the biological properties of distinct neuronal populations. Using bacterial artificial chromosome (BAC) transgenic mice that express EGFP-tagged ribosomal protein L10a in defined cell populations, we have developed a methodology for affinity purification of polysomal mRNAs from genetically defined cell populations in the brain. The utility of this approach is illustrated by the comparative analysis of four types of neurons, revealing hundreds of genes that distinguish these four cell populations. We find that even two morphologically indistinguishable, intermixed subclasses of medium spiny neurons display vastly different translational profiles and present examples of the physiological significance of such differences. This genetically targeted *t*ranslating *r*ibosome *a*ffinity *p*urification (TRAP) methodology is a generalizable method useful for the identification of molecular changes in any genetically defined cell type in response to genetic alterations, disease, or pharmacological perturbations.

INTRODUCTION

A century ago, Ramón y Cajal used Golgi staining to show that distinct cells called neurons are a major component of the mammalian central nervous system (CNS) (Ramón y Cajal et al., 1899). Today, hundreds of neuronal subtypes have been defined, but a molecular description of each subtype has been hampered by the same problems faced by Ramón y Cajal and his contemporaries: neuronal subtypes are highly heterogeneous and intermixed. Numerous attempts to extend microarray analysis of gene expression to defined cell populations in the CNS have relied upon the physical enrichment of target cell populations with laser-capture microdissection (LCM) or fluorescence-activated cell sorting (FACS) of acutely dissociated primary neurons. Unfortunately, these studies have been limited by stresses introduced during cellular isolation procedures, adaptations that occur upon loss of tissue-intrinsic signals, and the technical challenges associated with RNA purification from fixed tissue. To circumvent these problems, we have developed a direct, rapid affinity purification strategy for isolation of polysomal RNA from genetically targeted cell types.

We describe here a new *t*ranslating *r*ibosome *a*ffinity *p*urification (TRAP) methodology, which readily and reproducibly identifies translated mRNAs in any cell type of interest. This methodology involves expression of an EGFP-L10a ribosomal transgene, which enables tagging of polysomes for immunoaffinity purification of mRNA, in specific cell populations with bacterial artificial chromosome (BAC) transgenic mice, allowing CNS translational profiling from whole animals. Because of their ability to carry large pieces of regulatory information, BACs can be used to reproduce the expression pattern of a gene of interest. Indeed, a large number of BAC vectors driving expression in specific CNS cell types have been characterized as part of the Gene Expression Nervous System Atlas (GENSAT) project (Gong et al., 2003). BAC transgenic lines generated for the TRAP methodology, with the EGFP-L10a transgene, are referred to here as bacTRAP lines.

We illustrate the power of this approach in a study of four distinct neuronal populations. These include striatonigral and striatopallidal medium spiny neurons (MSNs), which are intermixed, indistinguishable in somatodendritic morphology, and of major interest because of their role in the etiology of various neurological and psychiatric diseases, including Parkinson's disease, schizophrenia, attention deficit hyperactivity disorder, drug addiction, and Huntington's disease. In the accompanying paper (Doyle et al., 2008), we describe the generation, characterization, and analysis of multiple additional genetically labeled lines as a resource for studies on a wide variety of CNS cell types.

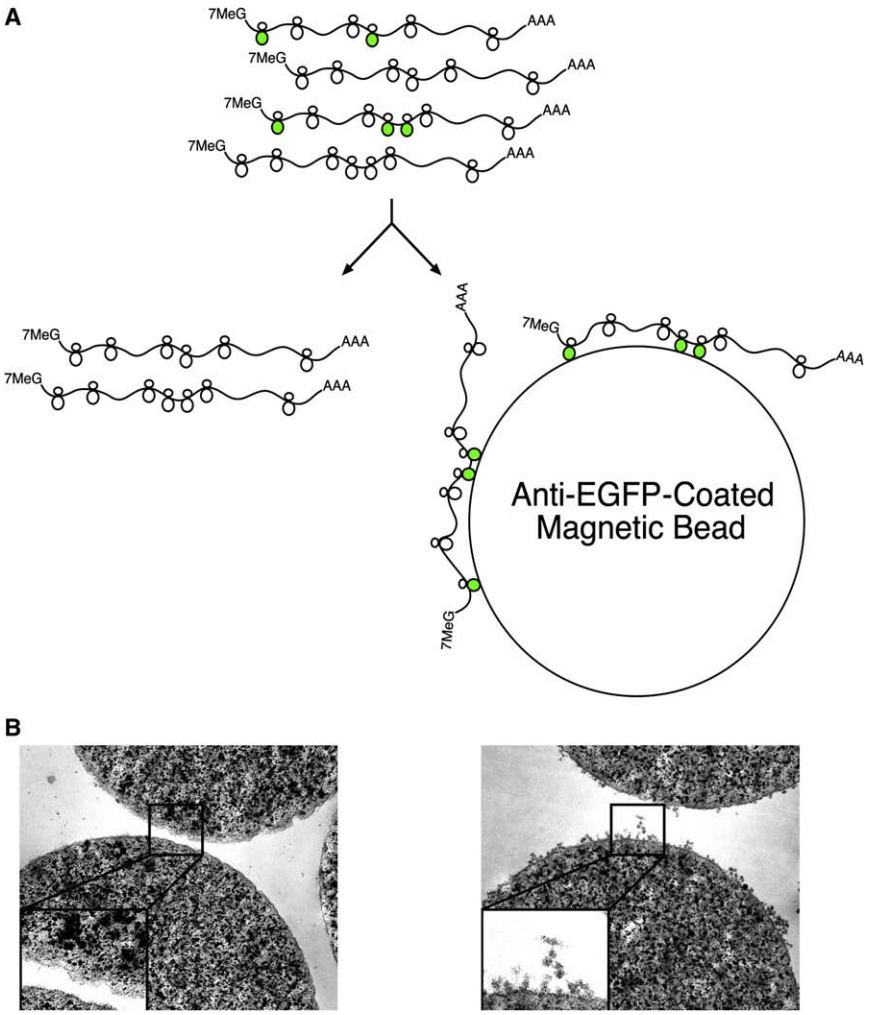

Figure 1. The TRAP Methodology

(A) Schematic of affinity purification of EGFP-tagged polysomes (originating from the target cell population; green polysomes) with anti-GFP antibody-coated beads.

(B) Transmission electron micrographs of anti-GFP-coated magnetic beads after incubation with extracts taken from HEK293T cells transfected with an empty vector (left panel) or the EGFP-L10a construct (right panel); images were acquired at 50,000× magnification, with inserts enlarged by a factor of 2.3×.

RESULTS

A Genetically Targeted Translational Profiling Methodology

Because all mRNAs translated into protein are at one point attached to a ribosome or polyribosome complex (polysome), we reasoned that an affinity tag fused to a ribosomal protein would allow isolation of bound mRNAs. We therefore screened fusions of ribosomal proteins with enhanced green fluorescent protein (EGFP) for efficient incorporation into polysomes to provide an immunoaffinity tag for all translated cellular mRNAs (schematic, Figure 1A). EGFP was chosen because preliminary screens using small epitope tags were unsatisfactory and because visualization of EGFP fluorescence provides a simple assay for proper expression and localization of the fusion protein. After dozens of candidate ribosomal protein fusions were tested, EGFP fused to the N terminus of the large-subunit ribosomal protein L10a (EGFP-L10a) was chosen because its nucleolar and cytoplasmic localization was consistent with incorporation into intact ribosomes and because immunoelectron microscopy data demonstrated its presence on polysomes (Figure S1 available online and data not shown). Prior to the production of bacTRAP transgenic mice, preliminary studies in HEK293T cells transfected with EGFP-L10a achieved rapid and specific immunoaffinity purification of polysomes (Figure 1B), overall copurification of ~10% of untagged ribosomal proteins and ribosomal RNA from cultures in which ~30% of cells expressed EGFP-L10a, and recovery observed for translated, and not untranslated, mRNAs (Table S1 and Figure S2). As further validation of the technique, measurements of the well-documented shift in translational efficiency of Ferritin mRNA in response to iron treatment were comparable with the TRAP methodology or traditional polysome gradient methods (Figure S2).

To genetically target expression of EGFP-L10a to defined CNS cell populations, we generated BAC transgenic mice. To tag polysomes in striatonigral and striatopallidal cells of the mouse striatum, we used homologous recombination in bacteria to place EGFP-L10a under the control of either the *Drd2* receptor (striatopallidal) or *Drd1a* receptor (striatonigral) loci in the appropriate BACs. Striatonigral MSNs send projection axons directly to the output nuclei of the basal ganglia, i.e., the substantia nigra and the internal segment of the globus pallidus (the entopeduncular nucleus in rodents), whereas striatopallidal MSNs send projection axons to the external segment of the globus pallidus. Mouse lines bearing the TRAP transgene (EGFP-L10a) were generated and screened by immunohistochemistry for appropriate expression of the transgene, as judged by known *Drd1a* and *Drd2* receptor expression patterns. The *Drd2* bacTRAP line CP101 showed highest transgenic EGFP-L10a expression in the dorsal and ventral striatum, olfactory tubercle, and hippocampus, as well as in the substantia nigra pars compacta and ventral tegmental area, as expected because of *Drd2* autoreceptor expression in dopaminergic cells (Figure 2A). The *Drd1a* bacTRAP line CP73 showed highest transgenic EGFP-L10a expression in the dorsal and ventral striatum, olfactory bulb, olfactory tubercle, and cortical layers 5 and 6 (Figure 2C). As expected for a ribosomal

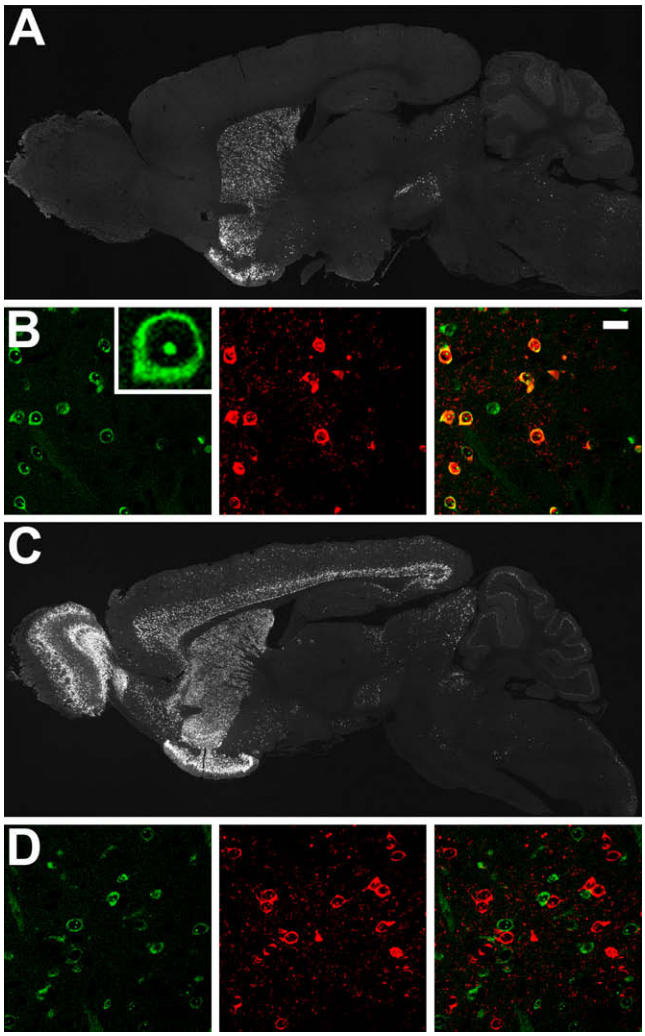

Figure 2. Expression of EGFP-L10a in *Drd1a* and *Drd2* bacTRAP Lines

(A) Immunohistochemistry to EGFP in adult sagittal sections from the *Drd2* bacTRAP line CP101.

(B) Characterization of *Drd2* bacTRAP line CP101 striatal MSN cells: direct EGFP fluorescence (left panel with high-magnification image insert), enkephalin immunohistochemical staining (middle panel), and merge (right panel, with 20 μm scale bar).

(C) Immunohistochemistry to EGFP in adult sagittal sections from the *Drd1a* bacTRAP line CP73.

(D) Characterization of *Drd1a* bacTRAP line CP73 striatal MSN cells: direct EGFP fluorescence (left panel), enkephalin immunohistochemical staining (middle panel), and merge (right panel).

protein fusion, EGFP fluorescence localized to the nucleoli and cytoplasm (Figure 2B). EGFP direct fluorescence coincident with enkephalin immunohistochemical detection (striatopallidal cell marker) was observed in striatal cells from the *Drd2* bacTRAP line but not the *Drd1a* bacTRAP line (Figures 2B and 2D), verifying correct BAC-mediated cell-type expression. Velocity sedimentation analysis of polysome complexes isolated from striatal extracts of both bacTRAP lines confirmed incorporation of the EGFP-L10a fusion protein into functional polysomes in vivo (Figure S3 and data not shown).

We next developed procedures for rapid extraction and immunoaffinity purification of the EGFP-tagged polyribosome complexes from intact brain tissue, which proved substantially more challenging than from transfected cells in culture. However, after several optimization steps (see the Experimental Procedures), highly purified RNA was consistently obtained from bacTRAP mouse brain tissue (Figure 3). Key steps of the purification protocol include rapid manual dissection and homogenization of the tissue, inclusion of magnesium and cycloheximide in the lysis buffer to maintain ribosomal subunits on mRNA during purification, inhibition of endogenous RNase activity, solubilization of rough endoplasmic reticulum-bound polysomes under nondenaturing conditions, use of high-affinity anti-EGFP antibodies, and the addition of high-salt washes after immunoaffinity purification to reduce background.

Translational Profiling of Striatonigral and Striatopallidal MSNs

Translational profiling analysis was performed with immunoaffinity-purified mRNA from adult striatonigral or striatopallidal bacTRAP mice. After two rounds of in vitro transcription, biotin-labeled antisense RNA (cRNA) was used to interrogate Affymetrix GeneChip Mouse Genome 430 2.0 arrays. Replicate bacTRAP samples collected from each line gave nearly identical genome-wide translational profiles (average Pearson correlation of 0.982 and 0.985 for striatonigral and striatopallidal samples, respectively). For each cell type, data were collected from three independent biological replicates, each prepared from a cohort of seven animals. Analysis of immunoaffinity-purified samples revealed no bias for mRNA length or abundance (Figure S4). Comparative analysis of these data (see the Experimental Procedures) revealed that all of the well-characterized, differentially expressed MSN markers (Gerfen, 1992) were enriched with the TRAP translational profiling approach: dopamine receptor 2 (*Drd2*) (36.6×), adenosine 2a receptor (*Adora2a*) (13.2×), and enkephalin (*Penk*) (7.5×) were enriched in the striatopallidal bacTRAP sample, whereas dopamine receptor D1A (*Drd1a*) (3.9×), substance P (*Tac1*) (3.6×), and dynorphin (*Pdyn*) (5.6×) were enriched in the striatonigral bacTRAP sample (Figure 3C and Table S2). We also confirmed four striatopallidal-enriched mRNAs (*Adk*, *Plxdc1*, *BC004044*, and *Hist1h2bc*), as well as six striatonigral-enriched mRNAs (*Slc35d3*, *Zfp521*, *Ebf1*, *Stmn2*, *Gnb4*, and *Nrxn1*) reported in a microarray study of FACS-isolated MSNs (Lobo et al., 2006) (Table S2). We further identified ~70 additional striatopallidal-enriched transcripts and more than 150 additional striatonigral-enriched transcripts (Table S2). To initially verify our data, we performed quantitative PCR assays using independent biological bacTRAP *Drd1a* and *Drd2* samples and a different cDNA amplification procedure (see the Supplemental Experimental Procedures). Differential translation of *Eya1*, *Isl1*, *Gng2*, and *Crym* in striatonigral MSNs and *Gpr6*, *Lhx8*, *Gpr88*, *Trpc4*, and *Tpm2* in striatopallidal MSNs was confirmed (Tables S3 and S4). These genes were selected because they represent both highly and moderately enriched messages.

Given the apparent enhanced sensitivity of our translational profiling method, we were next interested in large-scale

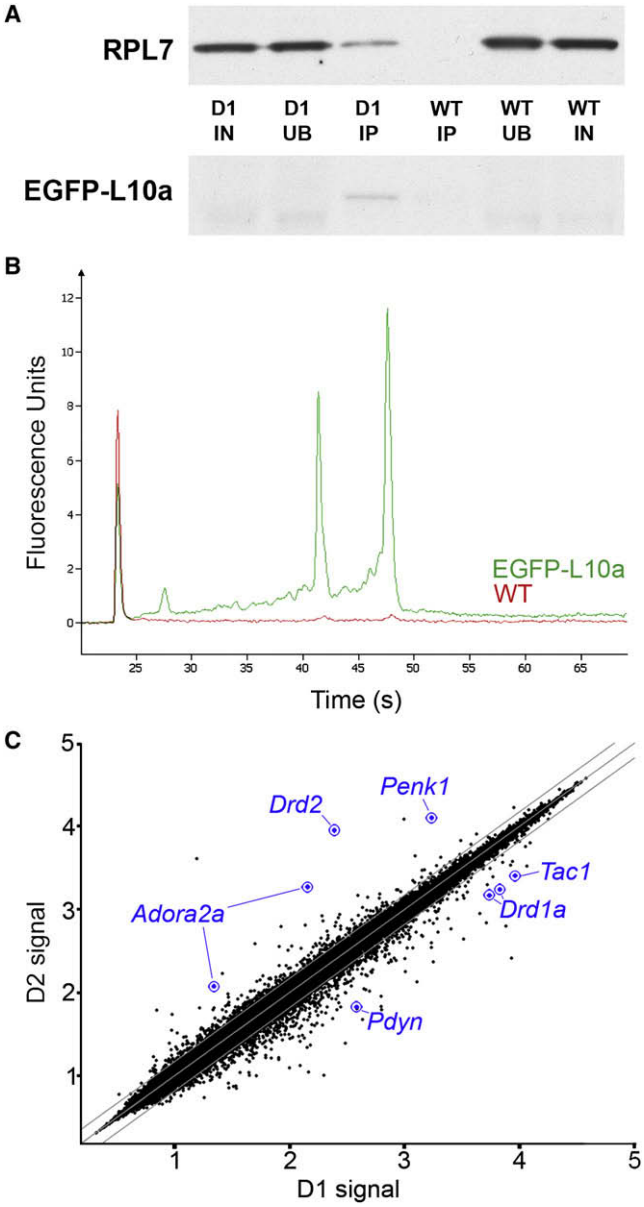

Figure 3. Protein and mRNA Purification from bacTRAP Lines

(A) Representative purification of EGFP-tagged L10a and copurification of untagged ribosomal protein L7 from *Drd1a* bacTRAP animals but not wild-type littermates (D1, samples from *Drd1a* bacTRAP mice; WT, samples from wild-type littermates; IN, 1% input; UB, 1% unbound; IP, 6.5% immunoaffinity-purified sample). EGFP-L10a signal is only present in the D1 IP lane because the IP samples were more concentrated relative to IN and UB.

(B) Representative purification of 18S and 28S rRNA from *Drd1a* bacTRAP transgenic animals (green) but not wild-type littermates (red) as detected by Bioanalyzer PicoChips (Agilent Technologies). 28S rRNA runs at ~47 s, 18S rRNA runs at ~43 s, and the Picochip marker peak runs at ~23 s.

(C) Normalized expression values from Affymetrix Mouse Genome 430 2.0 arrays are plotted for *Drd1a* and *Drd2* bacTRAP samples. The middle diagonal line represents equal expression, and lines to each side represent 1.5-fold enrichment in either cell population. Axes are labeled for expression in powers of 10. The probesets of well-studied genes known to be differentially expressed are represented in blue.

validation of the data with publicly available gene expression databases. Since in situ hybridization (ISH) alone cannot distinguish MSN subtypes, we pooled data from *Drd1a* and *Drd2* bacTRAP experiments and compared them to data collected from the total RNA of one whole brain (minus striatum) (Table S5). This analysis would be expected to identify most MSN-enriched transcripts, which can be evaluated in the ISH databases, whether or not they are differentially expressed in striatopallidal or striatonigral projection neurons. The analysis resulted in detection of several thousand translated mRNAs enriched in striatum relative to whole brain, including all previously well-known striatal-enriched genes: *Ppp1r1b/Darpp-32* (Walaas and Greengard, 1984), *Ptpn5/Step* (Lombroso et al., 1993), *Arpp-19* (Girault et al., 1990), *Arpp-21/RCS* (Ouimet et al., 1989), *Gnal/Golf* (Herve et al., 1993), *Rhes/Rasd2* (Falk et al., 1999), *Rgs9* (Gold et al., 1997), *Adcy5* (Glatt and Snyder, 1993), *Gng7* (Watson et al., 1994), *Rasgrp2* (Kawasaki et al., 1998), *Pde1b* (Polli and Kincaid, 1992), *Pde10a* (Fujishige et al., 1999), *Gpr88* (Mizushima et al., 2000), *Rarb* (Krezel et al., 1999), and *Strn4* (Castets et al., 1996), as well as the transcription factors *Foxp1*, *Foxp2* (Ferland et al., 2003), *Ebf1* (Lobo et al., 2006), and *Zfp503/Nolz* (Chang et al., 2004) (Table S5). Of the first 100 genes appearing in our MSN-enriched dataset, 26 were present in both of two major gene expression databases (the GENSAT/Brain Gene Expression Map [BGEM] and Allen Brain Atlas [ABA] ISH databases [http://www.ncbi.nlm.nih.gov/projects/gensat/; http://www.stjudebgem.org/] [Gong et al., 2003; Lein et al., 2007; Magdaleno et al., 2006]), and enriched striatal expression is evident for 22 of these genes (Table S5; Figure S5). Thus, TRAP translational profiling can provide a sensitive tool for discovery of large sets of translated messages in defined CNS cell populations.

To group striatonigral- and striatopallidal-enriched genes according to biological function, we looked for statistically overrepresented associations with Gene Ontology (GO) and Kyoto Encyclopedia of Genes and Genomes (KEGG) pathway terms (Tables S6–S11). GO terms delineate the known molecular functions, biological processes, and cellular localizations (components) for a particular gene (Ashburner et al., 2000), whereas KEGG pathways summarize known molecular interaction and reaction networks (Kanehisa, 1997). Some differentially translated mRNAs immediately predicted physiological differences between striatonigral and striatopallidal cells. For example, among striatopallidal-enriched mRNAs is *Gpr6* (Lobo et al., 2007), which encodes a G protein-coupled receptor for the lysophospholipid sphingosine 1-phosphate (S1P) (Ignatov et al., 2003). In heterologous expression systems, S1P activation of Gpr6 receptors induces intracellular Ca^{2+} release. As intracellular Ca^{2+} is a crucial regulator of neuronal physiology, we investigated whether striatopallidal enrichment of *Gpr6* reflects a differential response to S1P. To this end, BAC *Drd2* striatopallidal or BAC *Drd1a* striatonigral MSNs (expressing soluble EGFP) were identified in brain slices, patch clamped (Day et al., 2006), loaded with Alexa 594 to visualize dendrites, and loaded with Fluo-4 to monitor intracellular Ca^{2+} concentration (Figure 4A). A second pipette was then brought into close physical proximity to a dendrite, 60–80 μm from the soma, and used to apply S1P (Figures 4A and 4B). With the somatic membrane potential clamped at −70 mV, focal application of S1P consistently and reversibly increased

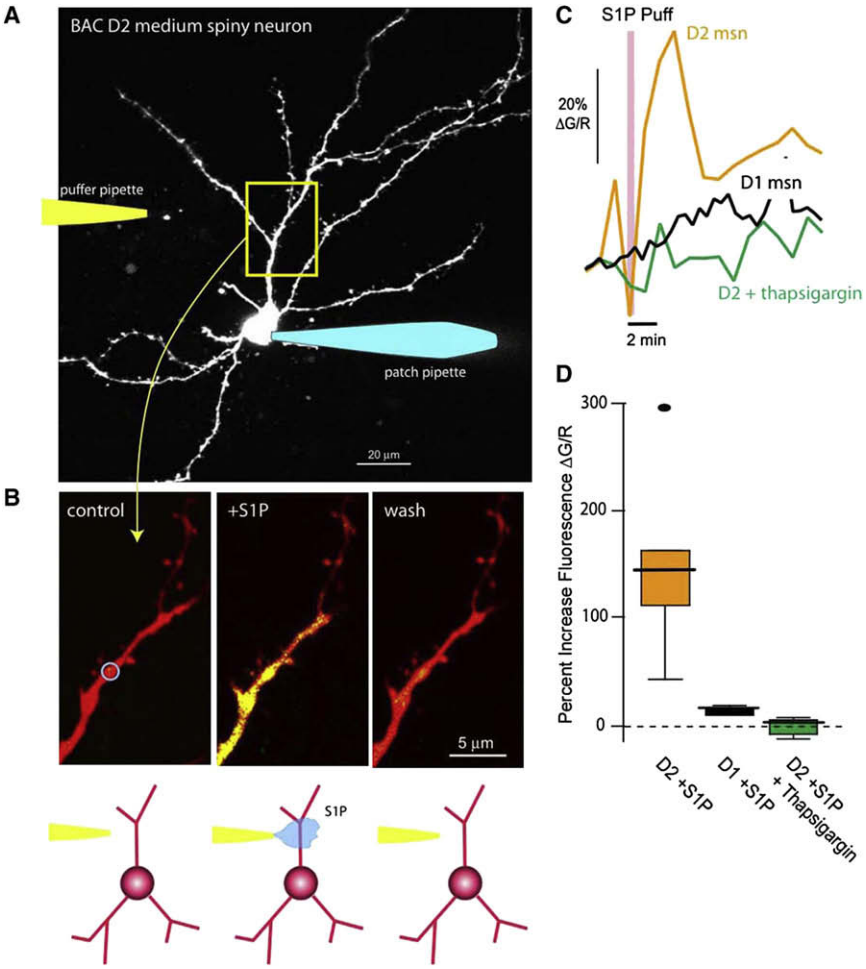

Figure 4. Functional Gpr6 Receptors Are Found in BAC *Drd2* Striatopallidal but not BAC *Drd1a* Striatonigral Medium Spiny Neurons

(A) Projection of an EGFP-labeled MSN from a BAC *Drd2* (D2) mouse. The cell was patched with a pipette containing Alexa 594 (50 μM) for visualization and Fluo-4 (200 μM) for measuring changes in intracellular Ca^{2+} (right). Cells were voltage clamped at –70 mV. A puffer pipette containing sphingosine 1-phosphate (S1P, 10 μM) was positioned near a dendrite, 60–80 μm from the soma (left/cartoon).

(B) High-magnification images of a dendritic segment (control, left panel) show an increase in Ca^{2+} associated with S1P application (S1P puff, center panel) that reversed with washing (wash, right panel). The change in Ca^{2+} was determined by calculation of the percent change in fluorescence of Fluo-4 relative to that of Alexa 594 (ΔG/R). The blue circle in the first panel indicates the analyzed region of interest (ROI).

(C) Time course showing the S1P induced increase in intracellular Ca^{2+} in the ROI from (B) (orange trace); similar recordings from BAC *Drd1a* (D1) MSNs (black trace) or 10 μM thapsigargin loaded BAC *Drd2* (D2) MSNs (green trace) did not reveal any significant changes in dendritic Ca^{2+} levels with S1P application.

(D) Box plot summarizing the S1P effects. Percent increase in fluorescence (ΔG/R) in BAC *Drd2* (D2) MSNs (median = 146%, range 44% to 294%, n = 6), BAC *Drd1a* (D1) MSNs (median = 17%, range 13% to 22%, n = 4), and thapsigargin-loaded BAC *Drd2* (D2) MSNs (median = 4%, range –9% to 10%, n = 4).

dendritic Ca^{2+} levels in BAC *Drd2* striatopallidal neurons (Kruskal-Wallis ANOVA, $p < 0.01$, n = 6) but not in BAC *Drd1a* striatonigral neurons (Kruskal-Wallis ANOVA, $p > 0.01$, n = 4) (Figures 4C and 4D). Depletion of intracellular Ca^{2+} stores with the Ca^{2+}-ATPase inhibitor thapsigargin abolished this response to S1P (Kruskal-Wallis ANOVA, $p > 0.01$, n = 4; Figures 4C and 4D). This striatopallidal-specific S1P response would be predicted to result in a decrease in threonine 34 (T34) phosphorylation of the centrally important regulatory protein DARPP-32 because of activation of the Ca^{2+} and calmodulin-dependent phosphatase calcineurin (Nishi et al., 1999) and/or inhibition of adenylyl cyclase type 5 (AC5; Adcy5) (Ishikawa et al., 1992; Glatt and Snyder, 1993). Indeed, a decrease in T34 DARPP-32 phosphorylation was seen after 5 min of S1P treatment of striatal slices (1.04 ± 0.17 normalized units at 0 min; 0.58 ± 0.24 normalized units at 5 min after S1P addition; one-tailed Mann-Whitney test, $p = 0.05$, n = 12). These data demonstrate the utility of TRAP translational profiling in identifying previously unrecognized functional differences in signaling responses between cell types.

Profiling of Cocaine-Induced Translational Changes

On the basis of the data above, it seemed likely that TRAP translational profiling could identify molecular responses to genetic, pharmacologic, or environmental changes in single cell types. To test this idea, we investigated changes in mRNA translation of MSNs upon pharmacological perturbation of dopaminergic signaling using cocaine, a competitive inhibitor of the dopamine transporter, which acts as a psychostimulant by elevating synaptic dopamine levels (Ritz et al., 1987; Di Chiara and Imperato, 1988). Adult mice were treated acutely or chronically with cocaine or saline and used for translational profiling of striatonigral (*Drd1a*) and striatopallidal (*Drd2*) MSNs. From this analysis, we identified hundreds of genes whose expression was increased or decreased in each cell type in response to cocaine (Tables S12 and S13). It is often difficult to directly compare gene expression data across drug administration experiments from published studies because of differences in strain background, dosing regimen, and assay sensitivity or array platform; in spite of this, we were able to identify various genes whose expression has been reported to be affected by cocaine administration, including: *Cartpt* (Douglass et al., 1995) (up in acute striatonigral; Table S12), *Fosb* (Hope et al., 1992) (up in acute striatonigral and striatopallidal and chronic striatonigral; Tables S12 and S13), *Homer1* (Brakeman et al., 1997) (up in acute striatonigral and striatopallidal, chronic striatonigral and striatopallidal; Tables S12 and S13), *Per2* (Yuferov et al., 2003) (up in acute

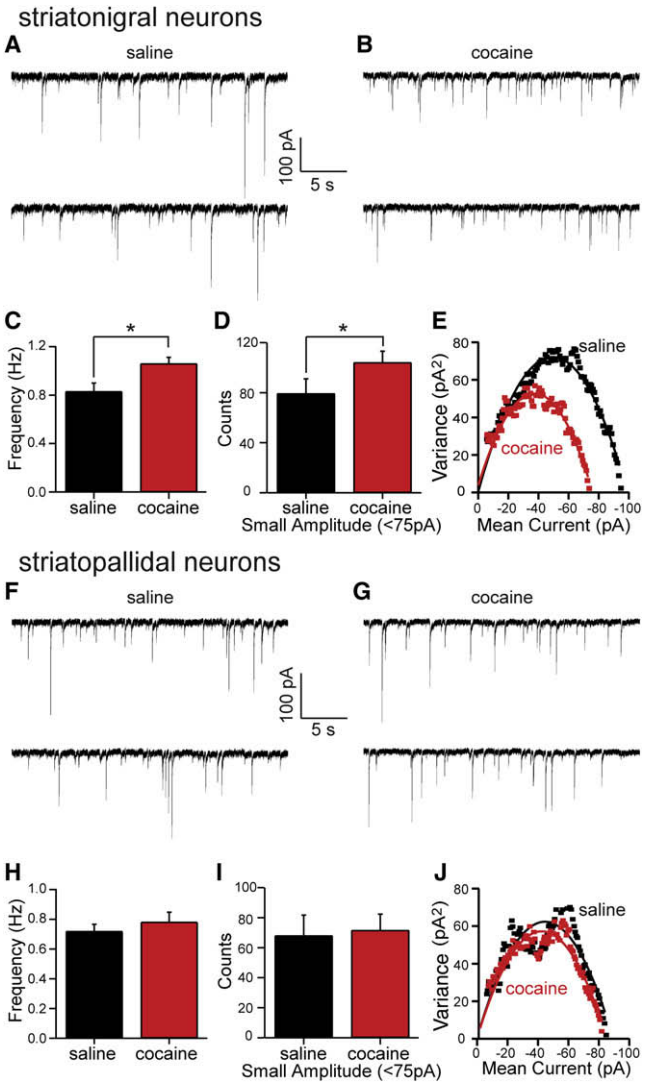

Figure 5. Cocaine Treatment Increases the Frequency of Small-Amplitude GABAergic mIPSCs in BAC *Drd1a* Striatonigral Medium Spiny Neurons

(A and B) Representative spontaneous mIPSCs traces from BAC *Drd1a* striatonigral neurons (expressing soluble EGFP under the *Drd1a* promoter) taken from mice treated for 15 days with saline (A) or cocaine (20 mg/kg/day) (B).

(C) Bar graph summary of mean mIPSC frequency showing a significant increase in BAC *Drd1a* striatonigral neuron mIPSCs frequency after cocaine treatment (saline = 0.83 ± 0.07 Hz, n = 22; cocaine = 1.04 ± 0.05 Hz, n = 26; $p < 0.05$, one-tailed t test).

(D) Bar graph summary showing that the number of small-amplitude mIPSCs (<75 pA) in equal length records (7 min) increased in BAC *Drd1a* striatonigral neurons after cocaine treatment (saline = 79.4 ± 8.2, n = 22; cocaine = 104.2 ± 6.3, n = 26; $p < 0.05$, one-tailed t test).

(E) Representative variance-mean current plots from saline-treated (black symbols) and cocaine-treated (red symbols) BAC *Drd1a* neurons suggesting that the cocaine-induced small-amplitude events arise from synapses that have fewer $GABA_A$ receptors (N) per synapse but receptors with an unchanged unitary receptor conductance (γ) (saline N = 33, γ = 31 pS; cocaine N = 29, γ = 31 pS; see Figures S6C and S6D for means).

(F and G) Representative spontaneous mIPSCs traces from BAC *Drd2* striatopallidal neurons after saline treatment for 15 days (F) and after cocaine treatment for 15 days (G).

striatopallidal and chronic striatonigral and chronic striatopallidal; Tables S12 and S13), *Vamp2* (McClung and Nestler, 2003) (up in chronic striatonigral; Table S13), *Kcnd2* (McClung and Nestler, 2003) (up in chronic striatonigral; Table S13), and *Zfp64* (McClung and Nestler, 2003) (up in acute striatopallidal, down in chronic striatopallidal; Tables S12 and S13).

We looked for statistically overrepresented GO and KEGG terms (Tables S14–S21) and noted that among the most significant GO biological processes altered in *Drd1a*-expressing striatonigral neurons upon chronic cocaine administration was the gamma-aminobutyric acid (GABA) signaling pathway (*Gabrb3*, *Gabra1*, *Cacnb4*, and *Gabra4*, Table S20). This finding is particularly interesting in light of positron emission tomography (PET) studies that have documented an enhanced sensitivity to the benzodiazepine lorazepam (binds GABA receptors) among chronic cocaine abusers (Volkow et al., 1998). For evaluation of the possible physiological significance of this upregulation, mice were chronically treated with cocaine or saline, and $GABA_A$ receptor function was assayed electrophysiologically. Cocaine treatment significantly increased the frequency of $GABA_A$ receptor miniature inhibitory postsynaptic currents (mIPSCs) in striatonigral neurons (saline = 0.83 ± 0.07 Hz, n = 22; cocaine = 1.04 ± 0.05 Hz, n = 26; $p < 0.05$, one-tailed t test; Figures 5A–5C). Visual inspection of representative records (as shown in Figures 5A and 5B) suggested that cocaine treatment increased the frequency of small-amplitude mIPSCs. To evaluate this possibility, we compiled the amplitude distribution of mIPSCs. The mode of this distribution was 75 pA in control recordings. Cocaine treatment appeared to shift the mode to smaller amplitudes. To determine whether the change in the distribution was significant, we compared equal length records for the number of submodal (<75 pA) and supramodal (≥75 pA) IPSCs. Cocaine treatment significantly increased the number of submodal events (saline = 79.4 ± 8.2, n = 22; cocaine = 104.2 ± 6.3, n = 26; $p < 0.05$, one-tailed t test; Figure 5D) but did not change the number of supramodal mIPSCs (saline = 81.9 ± 8.6, n = 22; cocaine = 80.8 ± 7.0, n = 26; $p > 0.05$, one-tailed t test; data not shown). The alterations in frequency and amplitude were not accompanied by a significant change in mIPSC kinetics (Figures S6A and S6B). Nonstationary noise analysis was also used to estimate single receptor conductance and the number of receptors per synapse (De Koninck and Mody, 1994). In neurons from saline-treated animals, the $GABA_A$ single receptor conductance was estimated to be 31 pS (Figure 5E; Figure S6C), a value very near that reported in other cell types (De Koninck and Mody, 1994; Kilman et al., 2002); cocaine treatment did not

(H) Bar graph summary of mean mIPSC frequency in saline- and cocaine-treated *Drd2* neurons, showing no effect of treatment condition (saline = 0.72 ± 0.05 Hz, n = 12; cocaine = 0.78 ± 0.07 Hz, n = 16; $p > 0.05$, one-tailed t test).

(I) Bar graph summary showing that the number of small-amplitude mIPSCs (<75 pA) in equal length records (7 min) was not altered by treatment condition in BAC *Drd2* neurons (saline = 68.1 ± 9.7, n = 12; cocaine = 71.7 ± 7.5, n = 16; $p > 0.05$, one-tailed t test).

(J) Representative variance-mean current plots showing that cocaine treatment did not change in the number of receptors per synapse or the unitary receptor conductance in BAC *Drd2* neurons (saline N = 34, γ = 31 pS; cocaine N = 33, γ = 30 pS; see Figures S7C and S7D for means).

All error bars represent standard error.

alter this value (saline $\gamma = 31.1 \pm 1.6$, n = 22; cocaine $\gamma = 30.8 \pm 1.2$, n = 26; $p > 0.05$, one-tailed t test; Figure 5E; Figure S6C). However, cocaine treatment did significantly reduce the estimated average number of receptors per synapse (saline N = 33.1 ± 1.4, n = 22; cocaine N = 29.3 ± 1.0, n = 26; $p < 0.05$, one-tailed t test; Figure 5E; Figure S6D). The most parsimonious interpretation of these results is that cocaine treatment leads to (1) the addition of small, dendritic $GABA_A$ synapses, resulting in an increase in mIPSC frequency, and (2) a decrease in the average number of receptors per synapse, due to dendritic synapses having fewer receptors than larger somatic synapses.

In contrast to *Drd1a*-expressing striatonigral neurons, *Drd2*-expressing striatopallidal neurons displayed no change in the frequency (saline = 0.72 ± 0.05 Hz, n = 12; cocaine = 0.78 ± 0.07 Hz, n = 16; $p > 0.05$, one-tailed t test; Figure 5H), amplitute (submodal mIPSCs, saline = 68.1 ± 9.7, n = 12; cocaine = 71.7 ± 7.5, n = 16; $p > 0.05$, one-tailed t test; Figure 5I; supramodal mIPSCs, saline = 59.1 ± 6.5, n = 12; cocaine = 63.3 ± 4.7, n = 16; $p > 0.05$, one-tailed t test; data not shown) and kinetics (Figures S7A and S7B) of $GABA_A$ mIPSCs after chronic cocaine treatment. Likewise, nonstationary noise analysis suggested that the average receptor conductance and number of receptors per synapse did not change in *Drd2*-expressing striatopallidal neurons after cocaine treatment (Figure 5J and Figures S7C and S7D). Taken together, these results demonstrate the physiological relevance of the selective cocaine-induced upregulation of mRNAs associated with $GABA_A$ receptors specific to *Drd1a*-expressing striatonigral neurons.

Although alterations in GABA release probability could also cause changes in mIPSC frequency, cocaine treatment altered the amplitude distribution of $GABA_A$ mIPSCs selectively in *Drd1a*-expressing striatonigral neurons, which would not be expected after a blanket increase in GABA release probability. The preferential increase in small-amplitude mIPSCs and the suggestion from nonstationary noise analysis that the average number of receptors per synapse fell in striatonigral neurons after cocaine treatment are consistent with the addition of small dendritic synapses, as opposed to larger somatic synapses (Kubota and Kawaguchi, 2000). Dendritic GABAergic synapses arise either from recurrent collaterals of other MSNs or from interneurons (Tepper et al., 2004). Definitively sorting out whether one or both of these classes contribute to the change in synaptic properties will require paired cell recordings and ultrastructural analysis (e.g., Koos et al., 2004; Kubota and Kawaguchi, 2000). Nevertheless, this upregulation may serve as an adaptive response to enhanced excitatory glutamatergic signaling in striatonigral neurons associated with the activation of D1 dopamine receptors by cocaine administration (Flores-Hernandez et al., 2002; Lee et al., 2006; Valjent et al., 2005; Wolf et al., 2004). The increased expression of physiologically active, inhibitory $GABA_A$ receptors in striatonigral cells could be a part of the molecular adaptations underlying the well-documented changes in sensitivity to cocaine seen among chronic abusers.

Translational Profiling of Cholinergic Motor Neurons and Purkinje Neurons

To determine whether the TRAP translational profiling methodology is generalizable, we produced cholinergic and Purkinje cell-specific bacTRAP lines. To this end, the EGFP-L10a transgene was placed under the control of the choline acetyltransferase (*Chat*) locus, specifically expressed in cholinergic cells in the CNS, or the Purkinje cell protein 2 (*Pcp2*) locus, specifically expressed in cerebellar Purkinje cells of the CNS (Oberdick et al., 1988). Consistent with known expression patterns, (Oh et al., 1992), the *Chat* bacTRAP line DW167 showed highest EGFP-L10a expression in cholinergic cells of the dorsal and ventral striatum, basal forebrain, brain stem, spinal cord, and medial habenula (Figure 6A), whereas the *Pcp2* bacTRAP line DR166 showed EGFP-L10a expression restricted to cells with characteristic Purkinje cell morphology (Figure 6C). Indirect immunofluorescence staining for Chat and Calbindin-D28K confirmed cell type-specific expression of the *Chat* and *Pcp2* lines, respectively (Figures 6B and 6D). One exception was in the pedunculopontine and laterodorsal tegmental nuclei, where only a minority of cholinergic cells were labeled with EGFP (data not shown).

Array data were collected from brain stem cholinergic motor neurons and from Purkinje cells with the *Chat* and *Pcp2* bacTRAP lines, respectively. Replicate bacTRAP samples gave nearly identical genome-wide translational profiles (average Pearson correlation of 0.982 and 0.997, respectively). We identified mRNAs enriched in each IP sample compared to an arbitrary reference sample (unbound fractions of the IPs) (Figures 7A–7D). Enrichment of cell-specific positive-control genes and exclusion of known negative-control genes (glial genes), were evident for each comparison (Figures 7A–7D). Venn diagrams constructed from the top 1000 enriched probesets from this analysis (Tables S22–S25) showed that the translational profiles of striatonigral and striatopallidal cells are more similar to each other than to translational profiles of either brain stem cholinergic cells or Purkinje cells (Figures 7E–7H).

DISCUSSION

TRAP translational profiling combines genetic targeting of an EGFP-L10a ribosomal fusion protein to specific cell populations; simple, rapid, affinity purification of mRNA; and microarray technology to identify translated mRNAs in situ. Unlike traditional approaches, it combines coincident detection of all translated mRNAs with cell-type specificity; thus, one quantitative TRAP experiment can replace thousands of high-throughput qualitative in situ hybridization runs and, further, can be repeated easily for each experimental condition. Second, the information obtained is cell type-specific while abrogating the physiologic adaptations and mRNA degradation that can occur during the lengthy cell separation procedures used in other approaches that sever neuronal axons and dendrites and disrupt tissue-intrinsic signaling. Third, because polysomes are stabilized with cycloheximide in the extraction buffers and during the affinity purification steps, redistribution of the affinity tag within the mRNA pool during polysome isolation is prevented, obviating the problems inherent in using less stable mRNA-binding proteins. Fourth, the use of established bacTRAP lines ensures that mRNA translation profiles can be reproducibly obtained and directly compared from the same cell population across experimental conditions. Crossing of these and other established bacTRAP lines to mouse models of various diseases

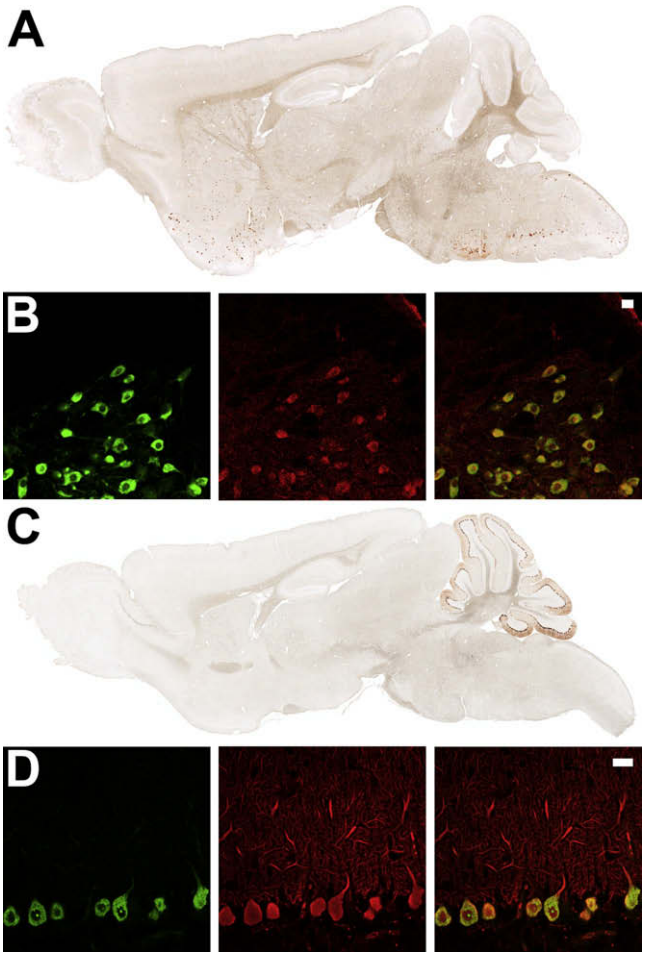

Figure 6. Expression of EGFP-L10a in the *Chat* and *Pcp2* bacTRAP Lines

(A) Immunohistochemistry to EGFP in adult sagittal sections from the *Chat* bacTRAP line DW167.

(B) Indirect immunofluorescent characterization of *Chat* bacTRAP line DW167 brain stem facial motor nucleus: EGFP staining (left panel), Chat staining (middle panel), and merge (right panel, with 20 μm scale bar).

(C) Immunohistochemistry to EGFP in adult sagittal sections from the *Pcp2* bacTRAP line DR166.

(D) Indirect immunofluorescent characterization of *Pcp2* bacTRAP line DR166 Purkinje cell neurons: EGFP staining (left panel), Calbindin-D28K staining (middle panel), and merge (right panel, with 20 μm scale bar).

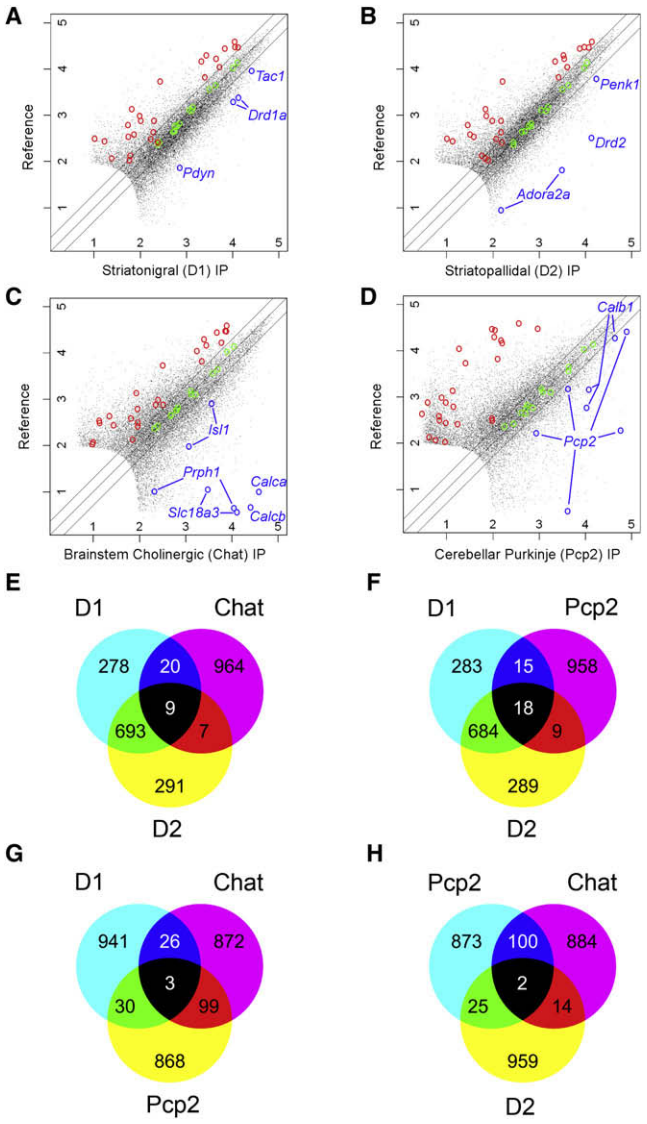

Figure 7. TRAP Profiles Recapitulate Known Cell-Specific Markers and Reveal New Ones for Four Distinct Cell Types

Scatterplots of *Drd1a* , *Drd2*, *Chat*, and *Pcp2* bacTRAP data compared to a reference mRNA sample reveal hundreds of genes enriched in each cell type (A–D). Green circles indicate Affymetrix biotinylated spike-in controls, blue circles indicate known cell-specific markers, and red circles indicate probesets for known glial genes (negative controls; Table S26). Lines on either side of the diagonal mark 2-fold enrichment. Axes are labeled for expression in powers of ten. Venn diagrams of the top 1000 enriched probesets (with expression value cutoff > 100) for each cell type reveal that each cell type has a unique pattern of enriched genes (E–H).

should greatly facilitate the elucidation of the molecular basis of disease phenotypes. Fifth, the use of EGFP as the affinity tag greatly facilitates anatomic studies of candidate bacTRAP mouse lines, as well as electrophysiological studies of each cell type. Finally, the profiling of only translated mRNA pools will more accurately reflect actual protein levels in a cell than does conventional gene expression profiling, which relies on total mRNA pools.

The TRAP approach thus overcomes limitations of previous mRNA-tagging methods that have targeted other RNA-binding proteins, of which only poly(A)-binding protein (PABP) has been used in vivo for tissue-specific studies (Roy et al., 2002; Kunitomo et al., 2005), and which requires crosslinking of the tagged PABP to mRNA (and its inherent artifacts) because of its loose association with mRNA. The use of tagged ribosomal proteins to purify translating polysomes from yeast as well as plant cells has recently been reported (Inada et al., 2002; Zanetti et al., 2005), although in these cases, cell-specific targeting to obtain cell-specific translational profiles was not attempted.

From our own experience, we know that adapting this methodology to cell-specific targeting is not trivial, particularly for applications in the mammalian CNS, with its far more difficult conditions of low expression, limited material, and contamination by blood, myelin, and other biological factors. As a result of the optimization reported here, the TRAP translational profiling methodology is now extremely robust to these conditions and broadly applicable (Doyle et al., 2008, accompanying paper).

Furthermore, the TRAP approach was able to identify all previously known, well-studied striatonigral- and striatopallidal-enriched genes (with one exception: the striatonigral-enriched muscarinic receptor M4 [*Chrm4*] [Ince et al., 1997], for which probesets on the Affymetrix Mouse 430 2.0 GeneChips gave very little signal; however, real-time PCR analysis of *Chrm4* expression demonstrated clear enrichment of *Chrm4* mRNA in our striatonigral bacTRAP cell sample [Table S3]). These results stand in distinction to a recent microarray study of FACS-sorted MSNs (Lobo et al., 2006), in which well-known positive-control genes (e.g., *Chrm4*, *Pdyn*, *Drd1a*, and *Drd2*) were not identified as differentially expressed on microarrays, and 16 of the 21 mRNAs reported in that study as striatopallidal-enriched in adult MSNs could not be confirmed in our analysis. Furthermore, we report here hundreds of distinguishing transcripts not identified in that study.

More importantly, our translational profiling analysis of striatal MSN subtypes has identified novel physiological differences between striatonigral and striatopallidal cells, which may provide new therapeutic targets for various neurological diseases associated with pathophysiology in the striatum. As one example, we demonstrate that striatopallidal cells selectively express *Gpr6* and that they correspondingly display a cell type-specific release of intracellular Ca^{2+} in response to sphingosine 1-phosphate. A second example of the distinct properties of these medically important cell types is provided by our studies of psychostimulant drug action, which give molecular and physiological evidence for upregulation of $GABA_A$ receptor subunits in striatonigral neurons after chronic cocaine administration.

The results presented here demonstrate that the TRAP translational profiling methodology provides an enabling technology for studies of the biology of specific cell types in even the most heterogeneous cell populations, such as those that occur in the CNS. We have identified numerous distinguishing molecular characteristics among four distinct neuronal populations, including two closely related, critical cell types and have demonstrated that the TRAP methodology can be employed to analyze physiological adaptations of specific cell types in vivo. An accompanying study (Doyle et al., 2008) has demonstrated the general applicability of the TRAP methodology by characterizing additional CNS cell types, each of which exhibits an enormously complex and cell-type specific molecular phenotype.

EXPERIMENTAL PROCEDURES

Generation of Mouse Lines

BAC transgenic mice were produced according to published protocols (Gong et al., 2003), with the exception that the EGFP-L10a transgene was used in place of EGFP.

Purification of mRNA from bacTRAP Mice

For striatonigral or striatopallidal translated mRNA purification, mice were decapitated, and the striata of seven bacTRAP transgenic mice were quickly manually dissected. Pooled striatal tissue was immediately homogenized in ice-cold polysome extraction buffer (10 mM HEPES [pH 7.4], 150 mM KCl, 5 mM $MgCl_2$, 0.5 mM dithiothreitol, 100 μg/ml cycloheximide, protease inhibitors, and recombinant RNase inhibitors) with a motor-driven Teflon glass homogenizer. Homogenates were centrifuged for 10 min at 2000 × *g*, 4°C, to pellet large cell debris, and NP-40 (EMD Biosciences, San Diego, CA) and 1,2-Diheptanoyl-*sn*-Glycero-3-Phosphocholine (DHPC; Avanti Polar Lipids, Alabaster, AL) were added to the supernatant at a final concentration of 1% and 30 mM, respectively. After incubation on ice for 5 min, the clarified lysate was centrifuged for 10 min at 13,000 × *g* to pellet unsolubilized material. Goat anti-GFP (custom made) -coated protein G Dynal magnetic beads (Invitrogen, Carlsbad, CA) were added to the supernatant, and the mixture was incubated at 4°C with end-over-end rotation for 30 min. Beads were subsequently collected on a magnetic rack, washed three times with high-salt polysome wash buffer (10 mM HEPES [pH 7.4], 350 mM KCl, 5 mM $MgCl_2$, 1% NP-40, 0.5 mM dithiothreitol, and 100 μg/ml cycloheximide) and immediately placed in TriZol-LS reagent (Invitrogen) and chloroform to extract the bound rRNA and mRNA from polysomes. After extraction, RNA was precipitated with sodium acetate and Glycoblue (Ambion, Austin, TX) in isopropanol overnight at −80°C, washed twice with 70% ethanol, resuspended in water, and further purified with an Rneasy Micro Kit (QIAGEN, Valencia, CA) with in-column DNase digestion. For the purification of translated mRNAs from brain stem cholinergic motor neurons (from the *Chat* bacTRAP line) or cerebellar Purkinje neurons (from the *Pcp2* bacTRAP line), nearly identical purifications as outlined above were performed, with a few minor modifications (see the Supplemental Experimental Procedures).

Microarray Data Normalization and Analysis

Three biological replicates were performed for each experiment. Quantitative PCR reactions were performed to validate array results with an independent biological source and amplification methodology (see the Supplemental Experimental Procedures). Striatonigral and striatopallidal GeneChip CEL files were imported into Genespring GX 7.3.1 (Agilent Technologies, Santa Clara, CA) and processed with the GC-RMA algorithm, and expression values on each chip were normalized to that chip's 50th percentile. Data were converted to $\log_2$ scale and filtered to eliminate genes with intensities in the lower range. A moderated two-tailed paired t test was performed with the Limma package from the Bioconductor project (http://www.bioconductor.org/). The p value of the moderated t test was adjusted for multiple hypothesis testing, controlling the false discovery rate (FDR) with the Benjamini-Hochberg procedure. We then selected all genes that had an FDR less than 0.1 (10%) and fold change larger than 1.5. Other comparisons were performed as described in detail in the Supplemental Experimental Procedures.

ACCESSION NUMBERS

The data discussed in this publication have been deposited in NCBI's Gene Expression Omnibus (GEO) (Edgar et al., 2002) and are accessible through GEO SuperSeries accession number GSE13394 (http://www.ncbi.nlm.nih.gov/geo/query/acc.cgi?acc=GSE13394).

SUPPLEMENTAL DATA

Supplemental Data include Supplemental Experimental Procedures, seven figures, and 26 tables and can be found with this article online at http://www.cell.com/supplemental/S0092-8674(08)01365-2.

ACKNOWLEDGMENTS

We thank Helen Shio for performing electron microscopy, Angus Nairn and Cordelia Stearns for striatal slice experimental data, and Joseph Doyle and Joseph Dougherty for bacTRAP data and analysis, as well as members of the P. Greengard, N. Heintz, GENSAT, G. Blobel, and R. Darnell laboratories

and Maxwell Heiman for comments and assistance. This work was supported by the National Institute on Drug Abuse (NIDA) fellowship 5F32DA021487 to M.H., German Research Foundation fellowship SCHA 1482/1-1 to A.S., National Institutes of Health/National Center for Research Resources grant 5UL1RR024143 to M.S.-F., National Institute of Neurological Disorders and Stroke grant NS34696 to D.J.S., grants from the F.M. Kirby Foundation, the Picower Foundation, the Jerry and Emily Spiegel Family Foundation, the Simons Foundation, the Peter Jay Sharp Foundation, and the Michael Stern Foundation, National Institute of Mental Health (NIMH) Conte Center grant MH074866 and NIDA grant DA10044 to P.G., the Simons Foundation, the Howard Hughes Medical Institute, the Adelson Medical Research Foundation, National Institute on Aging grant AG09464, and NIMH Conte Center grant MH074866 to N.H.

Received: April 22, 2008
Revised: July 18, 2008
Accepted: October 28, 2008
Published: November 13, 2008

REFERENCES

Ashburner, M., Ball, C.A., Blake, J.A., Botstein, D., Butler, H., Cherry, J.M., Davis, A.P., Dolinski, K., Dwight, S.S., Eppig, J.T., et al. (2000). Gene ontology: Tool for the unification of biology. The Gene Ontology Consortium. Nat. Genet. *25*, 25–29.

Brakeman, P.R., Lanahan, A.A., O'Brien, R., Roche, K., Barnes, C.A., Huganir, R.L., and Worley, P.F. (1997). Homer: A protein that selectively binds metabotropic glutamate receptors. Nature *386*, 284–288.

Castets, F., Bartoli, M., Barnier, J.V., Baillat, G., Salin, P., Moqrich, A., Bourgeois, J.P., Denizot, F., Rougon, G., Calothy, G., and Monneron, A. (1996). A novel calmodulin-binding protein, belonging to the WD-repeat family, is localized in dendrites of a subset of CNS neurons. J. Cell Biol. *134*, 1051–1062.

Chang, C.W., Tsai, C.W., Wang, H.F., Tsai, H.C., Chen, H.Y., Tsai, T.F., Takahashi, H., Li, H.Y., Fann, M.J., Yang, C.W., et al. (2004). Identification of a developmentally regulated striatum-enriched zinc-finger gene, Nolz-1, in the mammalian brain. Proc. Natl. Acad. Sci. USA *101*, 2613–2618.

Day, M., Wang, Z., Ding, J., An, X., Ingham, C.A., Shering, A.F., Wokosin, D., Ilijic, E., Sun, Z., Sampson, A.R., et al. (2006). Selective elimination of glutamatergic synapses on striatopallidal neurons in Parkinson disease models. Nat. Neurosci. *9*, 251–259.

De Koninck, Y., and Mody, I. (1994). Noise analysis of miniature IPSCs in adult rat brain slices: Properties and modulation of synaptic GABAA receptor channels. J. Neurophysiol. *71*, 1318–1335.

Di Chiara, G., and Imperato, A. (1988). Drugs abused by humans preferentially increase synaptic dopamine concentrations in the mesolimbic system of freely moving rats. Proc. Natl. Acad. Sci. USA *85*, 5274–5278.

Douglass, J., McKinzie, A.A., and Couceyro, P. (1995). PCR differential display identifies a rat brain mRNA that is transcriptionally regulated by cocaine and amphetamine. J. Neurosci. *15*, 2471–2481.

Doyle, J.P., Dougherty, J.D., Heiman, M., Schmidt, E.F., Stevens, T.R., Ma, G., Bupp, S., Shrestha, P., Shah, R.D., Doughty, M.L., et al. (2008). Application of a translational profiling approach for the comparative analysis of CNS cell types. Cell *135*, this issue, 749–762.

Edgar, R., Domrachev, M., and Lash, A.E. (2002). Gene Expression Omnibus: NCBI gene expression and hybridization array data repository. Nucleic Acids Res. *30*, 207–210.

Falk, J.D., Vargiu, P., Foye, P.E., Usui, H., Perez, J., Danielson, P.E., Lerner, D.L., Bernal, J., and Sutcliffe, J.G. (1999). Rhes: A striatal-specific Ras homolog related to Dexras1. J. Neurosci. Res. *57*, 782–788.

Ferland, R.J., Cherry, T.J., Preware, P.O., Morrisey, E.E., and Walsh, C.A. (2003). Characterization of Foxp2 and Foxp1 mRNA and protein in the developing and mature brain. J. Comp. Neurol. *460*, 266–279.

Flores-Hernandez, J., Cepeda, C., Hernandez-Echeagaray, E., Calvert, C.R., Jokel, E.S., Fienberg, A.A., Greengard, P., and Levine, M.S. (2002). Dopamine enhancement of NMDA currents in dissociated medium-sized striatal neurons: Role of D1 receptors and DARPP-32. J. Neurophysiol. *88*, 3010–3020.

Fujishige, K., Kotera, J., and Omori, K. (1999). Striatum- and testis-specific phosphodiesterase PDE10A isolation and characterization of a rat PDE10A. Eur. J. Biochem. *266*, 1118–1127.

Gerfen, C.R. (1992). The neostriatal mosaic: Multiple levels of compartmental organization in the basal ganglia. Annu. Rev. Neurosci. *15*, 285–320.

Girault, J.A., Horiuchi, A., Gustafson, E.L., Rosen, N.L., and Greengard, P. (1990). Differential expression of ARPP-16 and ARPP-19, two highly related cAMP-regulated phosphoproteins, one of which is specifically associated with dopamine-innervated brain regions. J. Neurosci. *10*, 1124–1133.

Glatt, C.E., and Snyder, S.H. (1993). Cloning and expression of an adenylyl cyclase localized to the corpus striatum. Nature *361*, 536–538.

Gold, S.J., Ni, Y.G., Dohlman, H.G., and Nestler, E.J. (1997). Regulators of G-protein signaling (RGS) proteins: Region-specific expression of nine subtypes in rat brain. J. Neurosci. *17*, 8024–8037.

Gong, S., Zheng, C., Doughty, M.L., Losos, K., Didkovsky, N., Schambra, U.B., Nowak, N.J., Joyner, A., Leblanc, G., Hatten, M.E., and Heintz, N. (2003). A gene expression atlas of the central nervous system based on bacterial artificial chromosomes. Nature *425*, 917–925.

Herve, D., Levi-Strauss, M., Marey-Semper, I., Verney, C., Tassin, J.P., Glowinski, J., and Girault, J.A. (1993). G(olf) and Gs in rat basal ganglia: Possible involvement of G(olf) in the coupling of dopamine D1 receptor with adenylyl cyclase. J. Neurosci. *13*, 2237–2248.

Hope, B., Kosofsky, B., Hyman, S.E., and Nestler, E.J. (1992). Regulation of immediate early gene expression and AP-1 binding in the rat nucleus accumbens by chronic cocaine. Proc. Natl. Acad. Sci. USA *89*, 5764–5768.

Ignatov, A., Lintzel, J., Kreienkamp, H.J., and Schaller, H.C. (2003). Sphingosine-1-phosphate is a high-affinity ligand for the G protein-coupled receptor GPR6 from mouse and induces intracellular Ca2+ release by activating the sphingosine-kinase pathway. Biochem. Biophys. Res. Commun. *311*, 329–336.

Inada, T., Winstall, E., Tarun, S.Z., Jr., Yates, J.R., 3rd, Schieltz, D., and Sachs, A.B. (2002). One-step affinity purification of the yeast ribosome and its associated proteins and mRNAs. RNA *8*, 948–958.

Ince, E., Ciliax, B.J., and Levey, A.I. (1997). Differential expression of D1 and D2 dopamine and m4 muscarinic acetylcholine receptor proteins in identified striatonigral neurons. Synapse *27*, 357–366.

Ishikawa, Y., Katsushika, S., Chen, L., Halnon, N.J., Kawabe, J., and Homcy, C.J. (1992). Isolation and characterization of a novel cardiac adenylylcyclase cDNA. J. Biol. Chem. *267*, 13553–13557.

Kanehisa, M. (1997). A database for post-genome analysis. Trends Genet. *13*, 375–376.

Kawasaki, H., Springett, G.M., Toki, S., Canales, J.J., Harlan, P., Blumenstiel, J.P., Chen, E.J., Bany, I.A., Mochizuki, N., Ashbacher, A., et al. (1998). A Rap guanine nucleotide exchange factor enriched highly in the basal ganglia. Proc. Natl. Acad. Sci. USA *95*, 13278–13283.

Kilman, V., van Rossum, M.C., and Turrigiano, G.G. (2002). Activity deprivation reduces miniature IPSC amplitude by decreasing the number of postsynaptic GABA(A) receptors clustered at neocortical synapses. J. Neurosci. *22*, 1328–1337.

Koos, T., Tepper, J.M., and Wilson, C.J. (2004). Comparison of IPSCs evoked by spiny and fast-spiking neurons in the neostriatum. J. Neurosci. *24*, 7916–7922.

Krezel, W., Kastner, P., and Chambon, P. (1999). Differential expression of retinoid receptors in the adult mouse central nervous system. Neuroscience *89*, 1291–1300.

Kubota, Y., and Kawaguchi, Y. (2000). Dependence of GABAergic synaptic areas on the interneuron type and target size. J. Neurosci. *20*, 375–386.

Kunitomo, H., Uesugi, H., Kohara, Y., and Iino, Y. (2005). Identification of ciliated sensory neuron-expressed genes in Caenorhabditis elegans using targeted pull-down of poly(A) tails. Genome Biol. *6*, R17.

Lee, K.W., Kim, Y., Kim, A.M., Helmin, K., Nairn, A.C., and Greengard, P. (2006). Cocaine-induced dendritic spine formation in D1 and D2 dopamine receptor-containing medium spiny neurons in nucleus accumbens. Proc. Natl. Acad. Sci. USA *103*, 3399–3404.

Lein, E.S., Hawrylycz, M.J., Ao, N., Ayres, M., Bensinger, A., Bernard, A., Boe, A.F., Boguski, M.S., Brockway, K.S., Byrnes, E.J., et al. (2007). Genome-wide atlas of gene expression in the adult mouse brain. Nature *445*, 168–176.

Lobo, M.K., Karsten, S.L., Gray, M., Geschwind, D.H., and Yang, X.W. (2006). FACS-array profiling of striatal projection neuron subtypes in juvenile and adult mouse brains. Nat. Neurosci. *9*, 443–452.

Lobo, M.K., Cui, Y., Ostlund, S.B., Balleine, B.W., and William Yang, X. (2007). Genetic control of instrumental conditioning by striatopallidal neuron-specific S1P receptor Gpr6. Nat. Neurosci. *10*, 1395–1397.

Lombroso, P.J., Naegele, J.R., Sharma, E., and Lerner, M. (1993). A protein tyrosine phosphatase expressed within dopaminoceptive neurons of the basal ganglia and related structures. J. Neurosci. *13*, 3064–3074.

Magdaleno, S., Jensen, P., Brumwell, C.L., Seal, A., Lehman, K., Asbury, A., Cheung, T., Cornelius, T., Batten, D.M., Eden, C., et al. (2006). BGEM: An in situ hybridization database of gene expression in the embryonic and adult mouse nervous system. PLoS Biol. *4*, e86.

McClung, C.A., and Nestler, E.J. (2003). Regulation of gene expression and cocaine reward by CREB and DeltaFosB. Nat. Neurosci. *6*, 1208–1215.

Mizushima, K., Miyamoto, Y., Tsukahara, F., Hirai, M., Sakaki, Y., and Ito, T. (2000). A novel G-protein-coupled receptor gene expressed in striatum. Genomics *69*, 314–321.

Nishi, A., Snyder, G.L., Nairn, A.C., and Greengard, P. (1999). Role of calcineurin and protein phosphatase-2A in the regulation of DARPP-32 dephosphorylation in neostriatal neurons. J. Neurochem. *72*, 2015–2021.

Oberdick, J., Levinthal, F., and Levinthal, C. (1988). A Purkinje cell differentiation marker shows a partial DNA sequence homology to the cellular sis/PDGF2 gene. Neuron *1*, 367–376.

Oh, J.D., Woolf, N.J., Roghani, A., Edwards, R.H., and Butcher, L.L. (1992). Cholinergic neurons in the rat central nervous system demonstrated by in situ hybridization of choline acetyltransferase mRNA. Neuroscience *47*, 807–822.

Ouimet, C.C., Hemmings, H.C., Jr., and Greengard, P. (1989). ARPP-21, a cyclic AMP-regulated phosphoprotein enriched in dopamine-innervated brain regions. II. Immunocytochemical localization in rat brain. J. Neurosci. *9*, 865–875.

Polli, J.W., and Kincaid, R.L. (1992). Molecular cloning of DNA encoding a calmodulin-dependent phosphodiesterase enriched in striatum. Proc. Natl. Acad. Sci. USA *89*, 11079–11083.

Ramón y Cajal, S., Pasik, P., and Pasik, T. (1899). Texture of the Nervous System of Man and the Vertebrates (Wien, New York: Springer).

Ritz, M.C., Lamb, R.J., Goldberg, S.R., and Kuhar, M.J. (1987). Cocaine receptors on dopamine transporters are related to self-administration of cocaine. Science *237*, 1219–1223.

Roy, P.J., Stuart, J.M., Lund, J., and Kim, S.K. (2002). Chromosomal clustering of muscle-expressed genes in Caenorhabditis elegans. Nature *418*, 975–979.

Tepper, J.M., Koos, T., and Wilson, C.J. (2004). GABAergic microcircuits in the neostriatum. Trends Neurosci. *27*, 662–669.

Valjent, E., Pascoli, V., Svenningsson, P., Paul, S., Enslen, H., Corvol, J.C., Stipanovich, A., Caboche, J., Lombroso, P.J., Nairn, A.C., et al. (2005). Regulation of a protein phosphatase cascade allows convergent dopamine and glutamate signals to activate ERK in the striatum. Proc. Natl. Acad. Sci. USA *102*, 491–496.

Volkow, N.D., Wang, G.J., Fowler, J.S., Hitzemann, R., Gatley, S.J., Dewey, S.S., and Pappas, N. (1998). Enhanced sensitivity to benzodiazepines in active cocaine-abusing subjects: A PET study. Am. J. Psychiatry *155*, 200–206.

Walaas, S.I., and Greengard, P. (1984). DARPP-32, a dopamine- and adenosine 3′:5′-monophosphate-regulated phosphoprotein enriched in dopamine-innervated brain regions. I. Regional and cellular distribution in the rat brain. J. Neurosci. *4*, 84–98.

Watson, J.B., Coulter, P.M., 2nd, Margulies, J.E., de Lecea, L., Danielson, P.E., Erlander, M.G., and Sutcliffe, J.G. (1994). G-protein gamma 7 subunit is selectively expressed in medium-sized neurons and dendrites of the rat neostriatum. J. Neurosci. Res. *39*, 108–116.

Wolf, M.E., Sun, X., Mangiavacchi, S., and Chao, S.Z. (2004). Psychomotor stimulants and neuronal plasticity. Neuropharmacology *47* (*Suppl 1*), 61–79.

Yuferov, V., Kroslak, T., Laforge, K.S., Zhou, Y., Ho, A., and Kreek, M.J. (2003). Differential gene expression in the rat caudate putamen after ''binge'' cocaine administration: Advantage of triplicate microarray analysis. Synapse *48*, 157–169.

Zanetti, M.E., Chang, I.F., Gong, F., Galbraith, D.W., and Bailey-Serres, J. (2005). Immunopurification of polyribosomal complexes of Arabidopsis for global analysis of gene expression. Plant Physiol. *138*, 624–635.